Direct Observation of One-Dimensional Diffusion and Transcription by *Escherichia coli* RNA Polymerase

Martin Guthold,*# Xingshu Zhu,*§ Claudio Rivetti,* Guoliang Yang,*§ Neil H. Thomson,¶ Sandor Kasas,¶ Helen G. Hansma,¶ Bettye Smith,¶ Paul K. Hansma,¶ and Carlos Bustamante*§‖

*Institute of Molecular Biology, #Physics Department, §Howard Hughes Medical Institute, and ‖Chemistry Department, University of Oregon, Eugene, Oregon 97403; and ¶Physics Department, University of California, Santa Barbara, California 93106 USA

ABSTRACT The dynamics of nonspecific and specific *Escherichia coli* RNA polymerase (RNAP)-DNA complexes have been directly observed using scanning force microscopy operating in buffer. To this end, imaging conditions had to be found in which DNA molecules were adsorbed onto mica strongly enough to be imaged, but loosely enough to be able to diffuse on the surface. In sequential images of nonspecific complexes, RNAP was seen to slide along DNA, performing a one-dimensional random walk. Heparin, a substance known to disrupt nonspecific RNAP-DNA interactions, prevented sliding. These observations suggest that diffusion of RNAP along DNA constitutes a mechanism for accelerated promoter location. Sequential images of single, transcribing RNAP molecules were also investigated. Upon addition of 5 μM nucleoside triphosphates to stalled elongation complexes in the liquid chamber, RNAP molecules were seen to processively thread their template at rates of 1.5 nucleotide/s in a direction consistent with the promoter orientation. Transcription assays, performed with radiolabeled, mica-bound transcription complexes, confirmed this rate, which was about three times smaller than the rate of complexes in solution. This assay also showed that the pattern of pause sites and the termination site were affected by the surface. By using the Einstein-Sutherland friction-diffusion relation the loading force experienced by RNAP due to DNA-surface friction is estimated and discussed.

INTRODUCTION

Since the invention of the scanning force microscope (SFM) (Binnig et al., 1982) researchers have steadily progressed toward the goal of imaging biological samples in aqueous environments and monitoring biochemical processes at nanometer resolution in real time (Drake et al., 1989; Rugar and Hansma, 1990; Hoh and Hansma, 1992; Bustamante et al., 1993, 1994). DNA was successfully imaged in contact mode SFM in air (Bustamante et al., 1992; Lyubchenko et al., 1992; Vesenka et al., 1992), water (Lyubchenko et al., 1993), and aqueous buffers (Hansma et al., 1993; Bezanilla et al., 1994a). The nonspecific binding of RNA polymerase (RNAP) to DNA molecules adsorbed onto mica was observed under aqueous conditions (Guthold et al., 1994). The recent development of tapping mode SFM in fluid (Dreier et al., 1994; Hansma et al., 1994; Putman et al., 1994; Han et al., 1996; Ratcliff et al., 1998; Guthold et al., 1999) has provided the means for less destructive imaging of biological specimens in liquid. By reducing lateral forces exerted by the tip on the sample, fluid tapping mode has been critical to the observation of DNA motion and enzymatic degradation of DNA (Bezanilla et al., 1994b; Bustamante et al., 1994), the analysis of supercoiled DNA (Lyubchenko and Shlyakhtenko, 1997) and Zn^{2+}-induced DNA kinks (Han et al., 1997). In the present study, this technique has been used to investigate the dynamic interactions of RNAP with DNA.

In *Escherichia coli*, transcription is carried out by a single enzyme, *E. coli* RNAP, and the rate of transcription initiation may, in part, be controlled by the rate at which the polymerase can find the promoter. That is, if the initial promoter binding step is not rapidly reversible on the time scale of subsequent isomerization steps of the promoter complex (Craig et al., 1998), an accelerated rate of promoter association will lead to accelerated transcription initiation, and thus more efficient transcription. In such a scenario, one problem that RNAP, and for that matter most other specific DNA-binding proteins, must solve is how to overcome the kinetic barrier of finding its specific binding site amid an excess of nonspecific DNA. Previously, it was proposed that the efficiency of a diffusion-controlled search could be enhanced by orders of magnitude if it were to take place in a space of lower dimensionality (Adam and Delbrück, 1968). Shortly afterward it was reported that *E. coli lac* repressor locates its target site at rates up to 1000 times faster than what could be accounted for by a three-dimensional diffusion-controlled search (Riggs et al., 1970). These and other authors then suggested that the search by DNA binding proteins for their specific site may be accelerated if they were able to first bind nonspecifically to DNA at any location, and then reach their target site by one-dimensional diffusion along the DNA (Richter and Eigen, 1974; Berg et al., 1981). According to these ideas, such a reduction in diffusion dimensionality could lead, under appropriate conditions, to greatly increased binding rates be-

Received for publication 11 March 1999 and in final form 8 July 1999.

Address reprint requests to Prof. Carlos Bustamante, Dept. of Molecular and Cell Biology, 337 Stanley Hall #3206, University of California at Berkeley, Berkeley, CA 94720-3206. Tel.: 510-643-9706; Fax: 510-642-5943; E-mail: carlos@alice.berkeley.edu.

Present address for Xingshu Zhu and Guoliang Yang: Dept. of Molecular and Cell Biology, University of California at Berkeley, Berkeley, CA 94720.

0006-3495/99/10/2284/11 $2.00

tween proteins and their cognate sites. This perception sparked the interest of scientists to demonstrate the existence and to elucidate the mechanisms of facilitated target location in DNA binding proteins.

Two investigations have used kinetic analysis to obtain evidence that RNAP may locate a promoter by one-dimensional diffusion along nonspecific DNA. In the first study (Singer and Wu, 1987), a rapid mixing/photocross-linking method was employed to monitor the time-dependent density of bound RNAP along a relaxed, circular DNA plasmid containing a single promoter. It was found that the occupancy by RNAP of the DNA segments near a promoter decreased faster than the occupancy of the segments farther away from the promoter. This phenomenon was interpreted as evidence that RNAP reached the promoter through one-dimensional diffusion along the DNA. In the second study (Ricchetti et al., 1988), the occupancy of DNA fragments carrying A1 promoters was measured as a function of the length of the downstream and upstream flanking sequence. A longer downstream flanking sequence increased the occupancy of the adjacent promoter in agreement with the sliding model. However, longer upstream sequences had surprisingly little effect on promoter occupancy.

In two recent investigations, fluorescence microscopy was used to observe the interactions of fluorescently labeled RNAP with DNA. In the first study (Kabata et al., 1993), super-intensified fluorescence microscopy was employed to visualize the movement of RNAP over combs of λ-DNA. A fraction of the RNAP molecules was seen to deviate from the direction of bulk flow and to move along the extended DNA molecules. This observation suggests that RNAP can slide along nonspecific DNA. However, in this experiment the RNAP was predominantly propelled by flow and was, therefore, not driven by thermal motion. In the second study (Harada et al., 1999), internal reflection fluorescence microscopy was used to observe the dissociation and association events of RNAP with different regions of a single λ-DNA molecule, which was suspended in laser tweezers. For AT-rich regions, fast and slow dissociation constants of 3.0 s^{-1} and 0.66 s^{-1} were determined respectively; for GC-rich regions a fast dissociation rate of 8.4 s^{-1} was measured. In a few instances, sliding of RNAP along the DNA was also observed in this study.

After RNAP has located a promoter, the protein-DNA complex undergoes a series of conformational changes that result in local unwinding of the DNA helix to expose the template strand (von Hippel et al., 1984; Leirmo and Record, 1990; Suh and Record, 1993; Craig et al., 1998). In the presence of nucleoside triphosphates (NTPs), synthesis of an RNA chain is initiated and the complex enters the elongation phase. During elongation, RNAP moves along the DNA template in a highly processive manner (Rhodes and Chamberlin, 1974), occasionally slowed by pauses (Chan and Landick, 1994), until a terminator is reached. Heretofore, nearly all investigations have used a large population of molecules because few techniques were available to study single transcription complexes. Hence, important properties of the individual molecules may have been lost in the time and population averages involved in bulk studies. Techniques capable of directly investigating the dynamics of individual molecules might, therefore, provide further insights into the mechanisms of transcription (Landick, 1997). In fact, several successful experiments on single transcription complexes have been reported recently. By using light microscopy, the shortening of the DNA template by a transcribing RNAP, which was fixed to a glass surface, has been monitored via a bead (Schafer et al., 1991). Moreover, the stall force of a transcribing RNAP was measured with laser tweezers and found to be ~14–30 pN at saturating NTP concentration (Yin et al., 1995; Wang et al., 1998b).

In the studies communicated here, scanning force microscope (SFM) imaging in liquid was used to investigate the dynamics of single, nonspecific, and specific RNAP-DNA complexes in real time. The first part of this paper describes the appropriate imaging conditions to carry out this work. In the second part, image sequences are shown that provide direct evidence that RNAP can diffuse along DNA (see also Bustamante et al., 1999). In the third part, image sequences of individual transcribing single RNAP molecules are investigated (see also Kasas et al., 1997) and the frictional loading force experienced by RNAP due to DNA-surface friction is estimated. Parallel biochemical experiments confirmed the activity and transcription rate determined from the image sequences.

MATERIALS AND METHODS

Sample preparation

A 1001-bp promoterless fragment, corresponding to the region from +12 to +1012 of the λP_{RM} gene, was used for the sliding studies. The fragment was amplified by PCR and gel-purified, followed by phenol/chloroform extraction and ethanol precipitation. A 946-bp promoterless fragment, which was used in some experiments, was obtained by *Eco*RI/*Pvu*PvuII digestion of pJES534, (gift of Dr. K. Rippe, German Cancer Research Center, Heidelberg, Germany), and further purified similarly to the 1001-bp fragment. Nonspecific binary complexes were formed by incubating 50–80 nM RNAP holoenzyme (σ70) (Epicentre Technologies, Madison, WI) and 10 nM nonspecific DNA fragment in transcription buffer (20 mM Tris or Hepes, 50 mM KCl, 5 mM $MgCl_2$, 1 mM 2-mercaptoethanol, pH 7.0) at room temperature for ~5 min.

The 1047-bp DNA template, which was used for the transcription studies, contains the λP_R promoter and the t_{R2} terminator (Fig. 3 *h*). It was amplified by PCR from plasmid pSAP (Dr. C. Rivetti) and purified by phenol/chloroform extraction, ethanol precipitation, and filtration through a Microcon 100 (Amicon, Inc., Beverly, MA). Stalled elongation complexes (A70) were formed according to Levin et al. (1987). RNAP holoenzyme (30 nM) was incubated with 10 nM DNA template in transcription buffer for 10 min at 37°C. Stalled elongation complexes were then formed by the addition of ATP, GTP, and UTP to a final concentration of 20 μM each and incubation for 10 min at room temperature.

SFM imaging in liquid

Nonspecific or stalled elongation complexes were diluted 5–10-fold in deposition buffer (4 mM Hepes, 1 mM KCl, 1 mM $MgCl_2$, pH 6.7–7.0), and 20 μl were deposited into the liquid cell O-ring, which had been placed

on freshly cleaved mica (Pelco Mica, Ted Pella Inc., Redding, CA). Without a prior rinsing or drying step, the SFM liquid chamber (glass cell, chamber volume ≈30 μl, Digital Instruments, Santa Barbara, CA), was placed on top of the sample drop. Using a flow apparatus (Thomson et al., 1996), imaging buffer (20 mM Tris-Cl, 5 mM KCl, 5 mM $MgCl_2$, 1 mM 2-mercaptoethanol, pH 7.0) was gently passed through the chamber for a few minutes to flush out the complexes that had not yet bound to the surface. In this flow apparatus, buffer containers (20 ml syringe tubes) were hung above the liquid chamber in order to obtain gravity-driven flow through the chamber. The outgoing tubes of the containers were connected to a six-port selection valve (valve and fittings; Upchurch Scientific, Oak Harbor, WA), which was connected through flexible tubing to the liquid chamber. This arrangement facilitated the switching between different buffers without disturbing the microscope. For the entire experiment, buffers were continuously flown through the chamber at a constant rate of ~0.3 ml/min. Note that constant flow was also maintained while capturing images. The flow was controlled with a micrometer screw clamping on the liquid cell inlet tube and the flow rate was determined by weighing the effluent with a balance (accuracy ±10 mg). When stable images were obtained, imaging was continued in transcription buffer for several minutes to establish optimal conditions for RNAP activity. For the transcription experiments, transcription buffer containing 5 μM NTPs was then flown through the chamber for the remainder of the experiment. Under these conditions, the temperature of the substrate in the liquid chamber was ~30°C as determined with a thermocouple that was attached to the mica surface. All images (256 × 256 pixels) were acquired at a rate of ~5 lines/s with a Nanoscope III SFM (Digital Instruments, Santa Barbara, CA). Electron-beam-deposited (EBD) tips (Keller and Chou, 1992) were used in all experiments. These tips were grown on gold-coated silicon nitride cantilevers (0.38 N/m) in an SEM (JSM-6300V, Joel U.S.A., Inc. Peabody, MA) at 20 kV and a working distance of 15 mm. The cantilever was driven at frequencies in the range of 10–15 kHz and drive amplitudes of 1–2 V. Free cantilever amplitudes were ~15–20 nm as determined from SFM force curves. The force exerted by the cantilever was minimized by imaging at the highest possible setpoint voltage, which was ~0.05 V less than the amplitude of the free oscillation close to the surface.

Two-dimensional diffusion coefficient of DNA molecules

For every frame in the sequence, the contour of each DNA molecule, L, was subdivided into n segments of length l, such that $nl = L$. The coordinates of the center of mass of each molecule, (x_{cm}, y_{cm}), were then determined from

$$(x_{cm}, y_{cm}) = \frac{\ell}{L}\left(\sum_{i=0}^{n} x_i, \sum_{i=0}^{n} y_i\right) \quad (1)$$

where x_i and y_i are the coordinates of the geometric center of the ith segment. The coordinates of the DNA contours were normalized relative to a fixed point in the image to eliminate the effect of lateral drift and scan motion. The two-dimensional diffusion coefficient of a molecule is then

$$D_{2D} = \frac{\sum_{k=1}^{N-1} (\Delta x_{cm,k})^2 + \sum_{k=1}^{N-1} (\Delta y_{cm,k})^2}{4(N-1)t} \quad (2)$$

where $\Delta x_{cm,k}$ and $\Delta y_{cm,k}$ represent the x and y excursions of the center of mass of a molecule during the time interval t. The values of D_{2D} determined for all molecules were then averaged to obtain the diffusion coefficient quoted in the text.

One-dimensional diffusion coefficient

The one-dimensional diffusion coefficient was calculated from

$$D_{1D} = \frac{\sum_{i=1}^{N-1} (\Delta \ell_i)^2}{2t} \quad (3)$$

where Δl_i is the change in DNA length measured from one DNA end to the polymerase during a time interval t. The values of D_{1D} determined for all complexes were then averaged to obtain the diffusion coefficient given in the text. The coordinates of the DNA contours were obtained from the images using the locally written image analysis program Alex (C. Rivetti and M. Young) which runs in the Matlab environment (The MathWorks, Inc., Natick, MA).

Biochemical transcription assay on mica surface

Stalled elongation complexes were formed as described above, except that [α-^{32}P]GTP (3000 Ci/mmol) was added to the reaction (final concentration 0.66 μM) before the addition of ATP, GTP, and UTP. The complexes were deposited onto mica disks and subjected to the same buffers used in the imaging experiments. After deposition, the disks were washed with 5 ml imaging buffer (wash 1) and then with 5 ml transcription buffer (wash 2) to rinse off complexes that had not yet bound stably to the surface. Transcription buffer containing 5 μM of all four NTPs was then applied to the mica disks, and the reaction was quenched after different lengths of time (see text) by rinsing with transcription buffer (no NTPs) (wash 3), and then adding gel loading buffer (7 M urea, 1X TBE, 0.5% SDS, 0.05% xylene cyanol, 0.05% bromphenol blue), which removed the sample from the mica disks. The washes ensured that only surface-bound complexes were analyzed in this transcription assay. The mica disks and all buffers were kept at 30°C according to the temperature measured inside the liquid cell under imaging conditions. The reaction products and the washes were analyzed by polyacrylamide gel electrophoresis (PAGE) in a denaturing 8% gel. The bands were quantified with a phosphoimager (STORM 860, Molecular Dynamics Inc. Sunnyvale, CA).

RESULTS

DNA diffusion on mica surface

Imaging the dynamic interactions between RNAP and DNA by SFM first required the resolution of an apparent paradox. Protein-DNA complexes had to be stably adsorbed onto the mica substrate so they could be imaged by the scanning tip, yet they had to be bound loosely enough to be able to diffuse on the substrate. To reconcile these conflicting requirements, initial experiments focused on finding imaging conditions in which the RNAP was stably bound to the mica, whereas the DNA molecules, although adsorbed onto the surface, were able to diffuse on it. It was found, as has also been reported previously, that binding of DNA to the mica substrate requires the presence of a divalent cation such as Mg^{2+}, Mn^{2+}, Ca^{2+}, Zn^{2+}, or Ni^{2+} (Guthold et al., 1994; Hansma and Laney, 1996) in the deposition buffer. It was also found that the concentration of monovalent cations in the deposition solution (not necessarily the imaging solution) should be less than about five times that of the divalent cations, independent of the total concentration of these ions. At higher monovalent ion concentrations in the deposition buffer, DNA molecules did not adsorb strongly enough to the mica to be imaged with the SFM. Deposition buffers with pH values below 6.5 also resulted in DNA adsorption too weak for imaging. Magnesium was chosen as the divalent ion in the present experiments because it is also essential for RNAP activity, while other cations are inhibitory to transcription (Zn^{2+}, Ni^{2+}) (Niyogi and Feldman, 1981) or induce kinks in the DNA (Zn^{2+},) (Han et al.,

1997). To minimize the lateral force exerted by the tip on the sample, images were acquired with tapping mode SFM in liquid. Furthermore, hydrophobic EBD tips, which appear to have minimal interactions with proteins and DNA, and which are often sharper than regular silicon nitride tips, were used in all experiments.

In Fig. 1 *a* the contours of 11 DNA molecules (1047 bp) from 11 sequentially recorded SFM images are superimposed to illustrate the DNA motion on the mica substrate. The coordinates of the molecules were taken with respect to a fixed feature in the image to eliminate the effect of drift and scan motion. The excursion of the center of mass of one DNA molecule is shown in the inset of Fig. 1 *a*. Fig. 1 *b* demonstrates that the mean diffusion distance, $\langle \Delta r \rangle$, is proportional to the square root of the time t, which is typical only for diffusion-controlled motion. The curve fit yielded a Pearson's R value of 99%. The average two-dimensional diffusion coefficient, $D_{2D} = \langle \Delta r^2 \rangle / 4t$, determined from 91 molecules of several different experiments, had a value of $\sim 7 \times 10^{-14}$ cm^2/s. The diffusion coefficient varied by approximately one order of magnitude among different experiments. This was probably due to the variability of the mica surface, which influences the strength of the mica-DNA interaction. Some of the motion of DNA on the surface could be due to the tip-DNA interaction. However, there is good evidence that the motion is mainly due to thermal energy. If the motion was caused by the tip it would be expected that the DNA moves mainly along the scan direction. This was usually not observed. More importantly, when the time between scans was increased, the mean square diffusion distance of the DNA molecules, $\langle \Delta r^2 \rangle$, also increased. Such behavior is typical only for thermal motion, but it would not be observed if the molecules were moved by the tip.

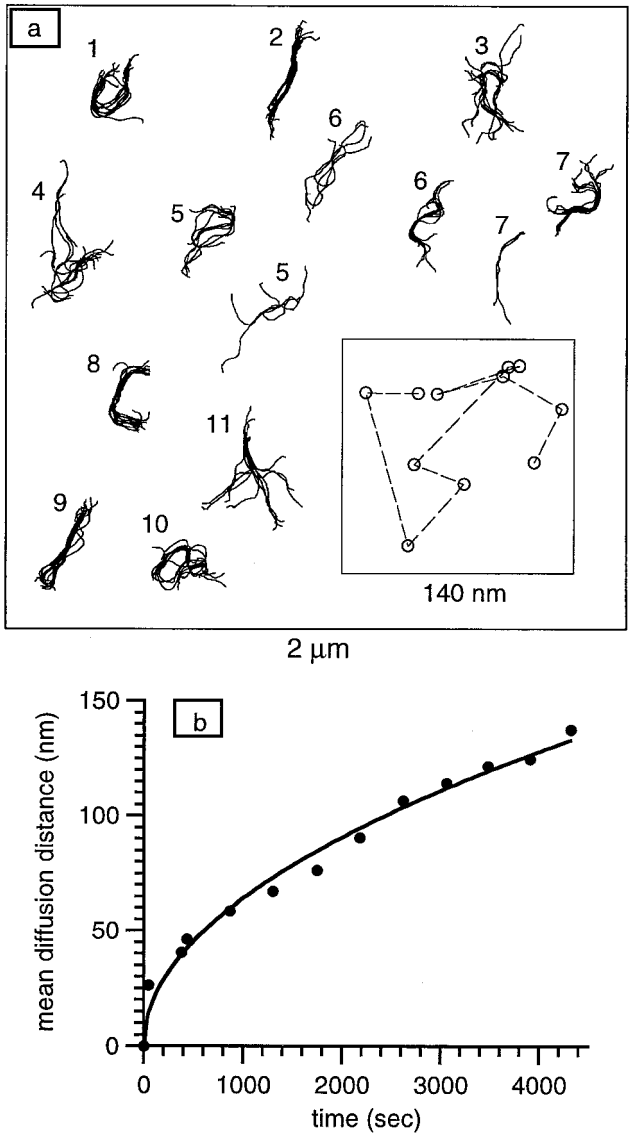

FIGURE 1 Two-dimensional diffusion of DNA on mica. (*a*) The contours of 11 DNA fragments (1047 bp) obtained from 11 consecutive SFM images (time interval between images, $t \approx 7$ min) are superimposed to illustrate the diffusion of the molecules on the surface. The inset shows the movement of the center of mass of one representative DNA molecule. To eliminate the *x-y* drift of the microscope between frames, the movement of the center of mass of each molecule was normalized to a fixed reference point on the surface. Image size: 2000 nm. (*b*) Plot of mean diffusion distance $\langle \Delta r \rangle$ vs. time t. A square root dependence, typical for diffusion-controlled motion, is seen.

RNAP diffusion along nonspecific DNA

Having obtained conditions in which DNA molecules can diffuse on the substrate while remaining adsorbed to it, experiments were designed to investigate whether RNAP can diffuse one-dimensionally along nonspecific DNA. Fig. 2 shows a typical time-lapse sequence of a nonspecific RNAP-DNA complex. In these images the polymerase appears as a white globular feature at the center of each image stably bound to the surface. The DNA molecule appears to be sliding back and forth beneath the enzyme (Fig. 2, *a–g*). In the last frame (Fig. 2 *h*), the protein has released the DNA. The position of the RNAP on the DNA fragment in successive images is depicted schematically in Fig. 2 *i*. Similar plots, obtained from >30 different imaging sequences, revealed that the relative position of the protein along the DNA is consistent with a random walk in one dimension. Fig. 2 *j* shows a plot of the mean diffusion distance along the DNA contour, $\langle \Delta l \rangle$, versus time t. It can be seen that $\langle \Delta l \rangle$ is roughly proportional to the square root of t, which is typical only for diffusion-controlled motion. The curve fit yielded a Pearson's R value of 89%. The average one-dimensional diffusion coefficient, $D_{1D} = \langle \Delta l^2 \rangle / 2t$, obtained from these images, had a value of $D_{1D} = 1.1 \times 10^{-13}$ nm^2/s. The average lifetime of these nonspecific RNAP-DNA complexes on the surface was ~600 s, which is large compared to nonspecific complexes in solution (see Discussion).

Effect of heparin on nonspecific complexes

The spatial resolution of the SFM images is generally not sufficient to unequivocally identify these pairs as nonspe-

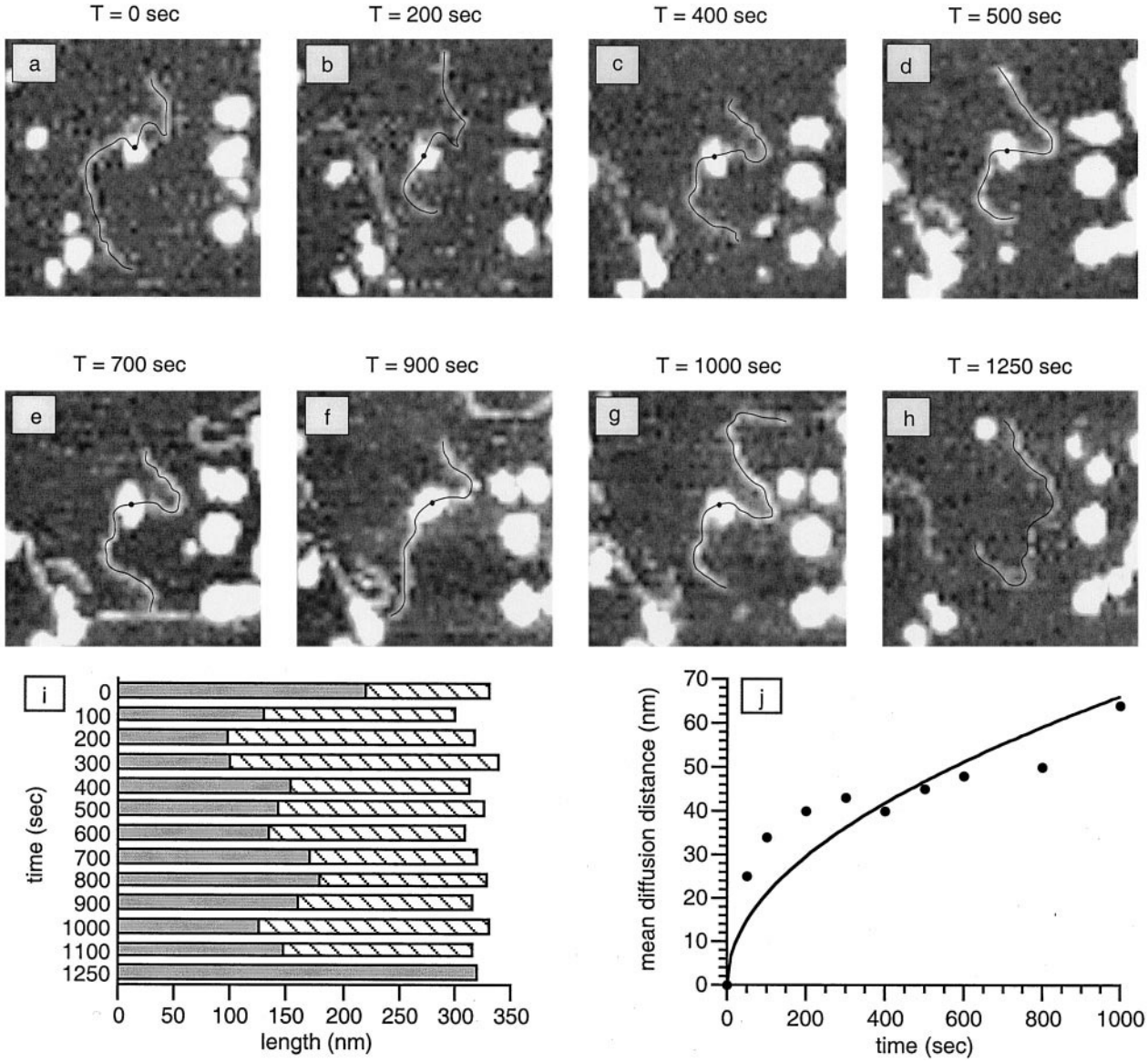

FIGURE 2 One-dimensional diffusion of nonspecific binary complexes of RNAP along the DNA. (*a–h*) SFM time-lapse sequence of RNAP sliding. Polymerase appears to slide back and forth several times along the DNA molecule before it is released. The elapsed time after the initial observation of the complex is indicated above each image. The DNA contour is traced with a thin line and the center of the RNAP is marked with a dot. Image size: 350 nm. The height color code ranges from 0 nm (*black*) to 5 nm (*white*). (*i*) Bar plot representation of the length of the two DNA arms (*hatched* and *solid bars*) in 13 sequential images. (*j*) Plot of mean diffusion distance $\langle \Delta l \rangle$ vs. time *t*. A square root dependence, typical for diffusion-controlled motion, is seen.

cific complexes. Therefore, a control experiment was carried out to demonstrate that these complexes are indeed nonspecific complexes and not just the DNA and RNAP positioned in close proximity by chance. Heparin, a polyanion and DNA analog, is known to disrupt the relatively weak nonspecific RNAP-DNA interaction and to inhibit DNA binding of RNAP (Walter et al., 1967; Kadesch et al., 1980; Schlax et al., 1995). Accordingly, if these complexes were true nonspecific complexes, subjection to heparin will have a deleterious effect on sliding. However, heparin will have *no* effect if RNAP and DNA would not be interacting with each other, or if the complexes were the heparin-resistant tight-binding kind (Kadesch et al., 1980). The effect of heparin on diffusion of RNAP along a DNA fragment was tested on 14 sliding complexes. When these complexes were exposed to heparin, 13 of them dissociated right after the arrival of heparin in the liquid cell and no re-association was observed, thus significantly reducing the lifetime of these complexes. Only one of them seemed to stay bound for a longer time. The fact that heparin had such a marked effect on these complexes implies that the DNA and RNAP were interacting nonspecifically with each other.

Image sequences of single transcribing RNAP molecules

To study the dynamics of a transcribing RNAP, a fragment containing the λP_R promoter and t_{R2} terminator was used

(Fig. 3 *h*). Stalled elongation complexes were formed in solution and adsorbed onto a mica surface. To capture various intermediates of the elongation process, the rate of transcription was adjusted by lowering the nucleotide concentration to 5 μM. Under these conditions, NTP binding becomes the rate-limiting step of the reaction. Assuming a simple Michaelis-Menten model, the steady-state initial rate of elongation is given by $v_0 = v_{max} \cdot [NTP]/(K_m + [NTP])$. With a maximum velocity of $v_{max} = 50$ nt/s (Kassavetis and Chamberlin, 1981) and a Michaelis constant of $K_m = 50$ μM a rate of $v_0 \approx 5$ nt/s is obtained for an NTP concentration of [NTP] = 5 μM. Fig. 3 is a time-lapse sequence of a transcribing RNAP complex imaged in transcription buffer with the SFM. A stalled elongation complex, identified by the location of the polymerase on the DNA template, is shown shortly before the addition of NTPs to the liquid cell (Fig. 3 *a*). In several images before Fig. 3 *a*, the arms of the DNA on both sides of the polymerase diffused laterally on the mica surface but did not move through the polymerase in either direction, indicating a stable stalled elongation complex. Upon nucleotide injection, RNAP began to thread the DNA template in a processive and unidirectional manner (Fig. 3, *b–g*) toward the shorter arm of the DNA, consistent with the orientation of the promoter in the template. After transcription, RNAP usually released the DNA. An analysis of the transcription rates from a total of 20 complexes yielded an average value of 1.5 $\pm$ 0.8 nt/s.

Biochemical transcription assay on mica surface

The RNA transcript was not unequivocally identifiable in the images. Presumably, it attained a compact secondary structure that remained in contact with the RNAP, and perhaps could not be resolved due to the apparent broadening of the RNAP by the scanning tip (Bustamante and

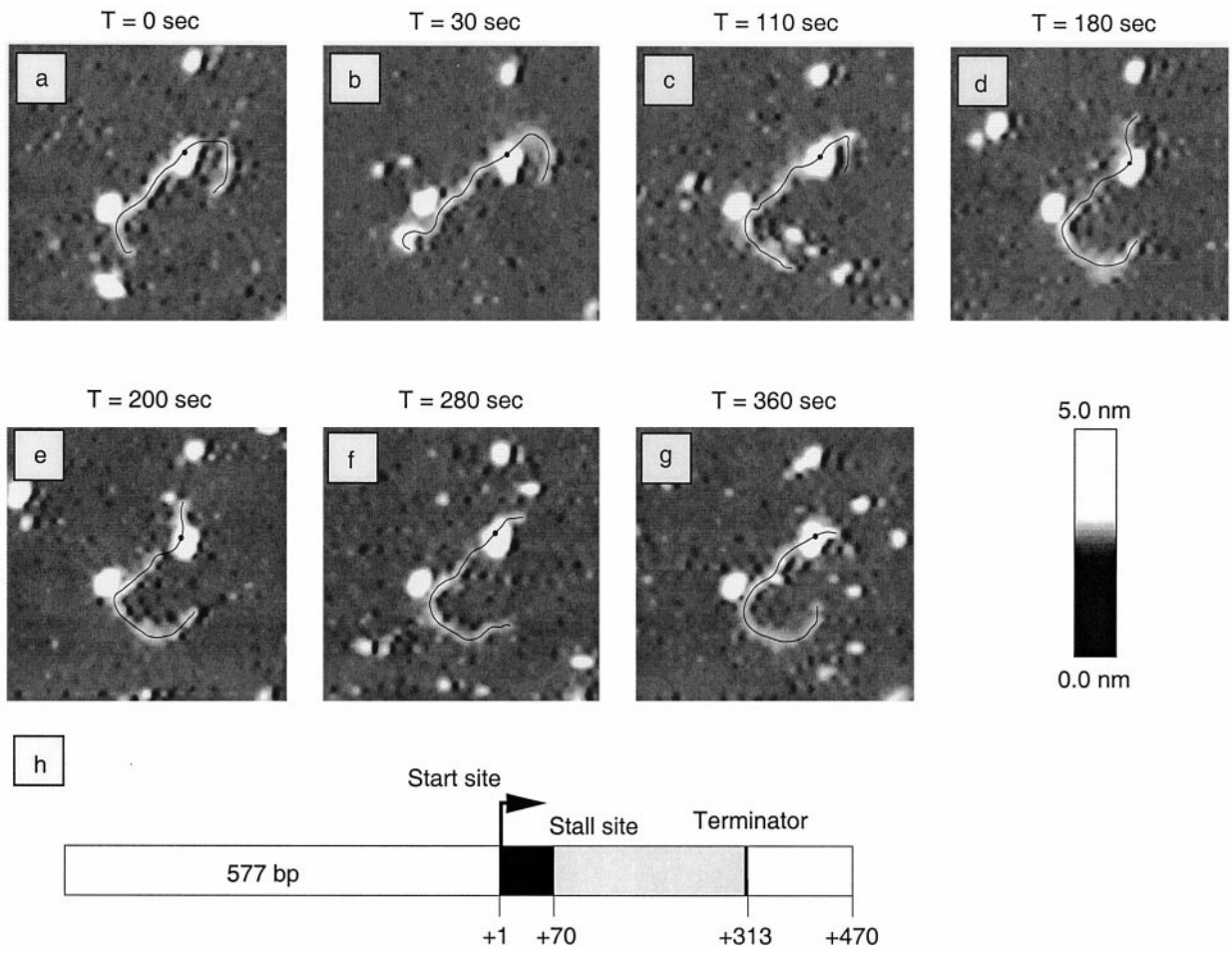

FIGURE 3 SFM time-lapse sequence of a transcribing RNAP. (*a*) Image of a stalled elongation complex (A70), as judged from the length of the DNA arms, before the injection of NTPs into the liquid cell. (*b–g*) Consecutive images after transcription was resumed by flowing 5 μM NTPs in transcription buffer through the liquid cell. During transcription, which proceeds toward the shorter arm, the RNAP remained stably bound to the surface while the DNA was pulled through the protein. The DNA contour is traced with a thin line and the center of the RNAP is marked with a dot. Image size and colors as in Fig. 2. (*h*) Map of the 1047 bp DNA template used in the transcription experiments. The sequence of the coding strand allows the formation of stalled elongation complexes (A70) with a 70 nucleotide-long transcript in a transcription reaction lacking CTP. The location of the stalling site on the template is asymmetric (577 bp vs. 470 bp) so that stalled elongation complexes and the direction of transcription can be identified in the images.

Keller, 1995). A biochemical control experiment was, therefore, designed to investigate the activity and transcription rate of mica-bound complexes. Stalled elongation complexes prepared with a radiolabeled transcript were deposited onto mica and subjected to the same buffer conditions and temperature as in the imaging experiments. Fig. 4 *a* compares the activity and transcription rates of these mica-bound complexes with those determined for complexes in solution. A quantitative analysis of the bands revealed that ~40–50% of the complexes on the surface and ~75–80% of the complexes in solution are able to extend the transcript. Hence, as judged by this criterion, the activity of the complexes on the surface is similar, but somewhat lower than the activity of the complexes in solution. When comparing the transcription rates of solution and surface-bound complexes, a larger difference is apparent. The complexes in solution transcribe at a rate of ~5 nt/s, whereas the surface-bound complexes transcribe at a rate of ~1 nt/s. At higher NTP concentrations, the transcription rates for both complexes increased, but the rate for complexes on the surface remained lower than the rate for complexes in solution. The pattern of pauses and termination at the t_{R2} site are also affected by the surface. Although many pause sites are the same for surface-associated complexes and solution complexes, there are also distinct differences. One might expect that surface-bound complexes would just have more pauses because RNAP has to overcome the additional drag force acting on the DNA. However, it appears that either complex has some unique pause sites that are not very pronounced in the other one. Moreover, surface-associated complexes apparently yield different transcripts than the correct, full-length transcript, and seem to produce significant quantities of transcripts that are longer than the correct full-length transcripts (see Discussion).

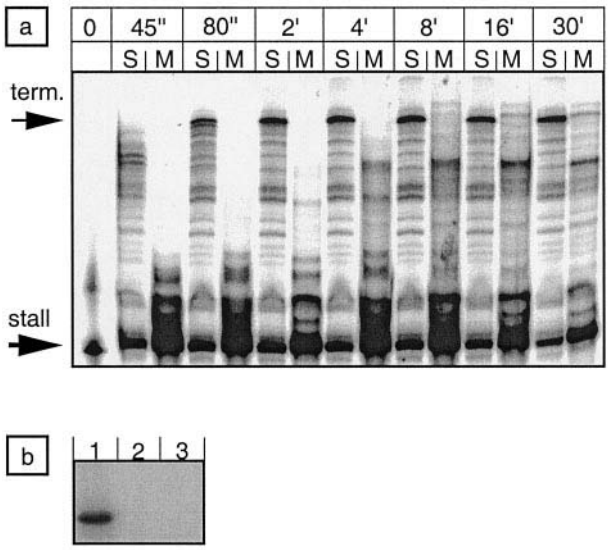

FIGURE 4 Activity and transcription rates of stalled elongation complexes in solution and on a mica surface. (*a*) Stalled elongation complexes in solution (S) or on a mica surface (M) were chased with 5 μM NTPs in transcription buffer. The reaction was quenched with gel loading buffer at the indicated times, and the products were analyzed using denaturing PAGE. *Lane 1:* 70 nt RNA from unchased stalled elongation complexes; *lanes 2–15:* time course of transcription elongation for solution (S) and mica-bound (M) stalled elongation complexes. A quantitative analysis of the bands revealed that ~40–50% of the complexes on the surface, as compared to ~75–80% of the complexes in solution, were able to extend the transcript. The rate of transcription is ~1 nt/s and 5 nt/s for the surface-bound complexes and complexes in solution, respectively. (*b*) Analysis of the three washes applied to surface-bound complexes. About 70% of the total number of complexes deposited were rinsed off in the first wash (*lane 1*). They had not yet bound to the surface. No complexes were detached from the surface in the two subsequent washes (*lanes 2* and *3*) indicating that once the complexes had bound to the surface they remained adsorbed to it.

To verify that the measured transcriptional activity corresponded to surface-bound complexes and not to complexes that had detached from the surface, the sample was rinsed twice after the deposition and once after the addition of nucleotides. These washes were then analyzed by denaturing PAGE. Fig. 4 *b* shows that ~70% of the total number of complexes were rinsed off in the first wash; these complexes had not yet bound to the surface. Both subsequent washes were completely clear, indicating that the complexes remained adsorbed to the surface once they had bound to it. The radiolabeled transcript was removed from the surface using denaturing gel loading buffer containing 0.5% SDS and analyzed by PAGE.

DISCUSSION

The goal of this study was to image and characterize the dynamics of specific and nonspecific RNAP-DNA complexes. The initial challenge in these experiments was to find imaging conditions in which, at the same time, 1) RNAP be active on a surface suitable for SFM imaging, 2) DNA fragments be stably adsorbed onto the surface so that they can be imaged by the scanning tip, and 3) the DNA fragments be able to diffuse laterally on the surface. The conditions described in this paper satisfy all these requirements.

Two-dimensional diffusion of DNA

The behavior of the DNA on the substrate can be explained by a model for the equilibration of DNA molecules on a mica surface (Rivetti et al., 1996). The mica substrate is described as an array of discrete binding sites capable of interacting with the many segments of a DNA polymer. The DNA segments are able to exchange among the various binding sites; the rate of this exchange, and thus the magnitude of the diffusion constant, is determined by the activation energy to move one segment from one binding site to another with no net change in binding energy. The dynamics of the molecules on the surface are thus controlled by the density and strength of binding sites and the length of the polymer (Bustamante and Rivetti, 1996; Rivetti et al., 1996). According to this model, complete detachment of a molecule from the surface is thermodynamically unfavor-

able, as it would require the simultaneous breaking of many molecule-surface interactions.

RNAP sliding

In the present study, sequential SFM images of single RNAP molecules sliding along individual DNA fragments were recorded and analyzed. These images demonstrate that RNAP can use one-dimensional diffusion along nonspecific DNA to accelerate the search for promoters. The ability of heparin to disrupt the sliding process and, thereby, reduce the mean diffusion time of the polymerase on the DNA, supports the identification of the RNAP-DNA complexes as nonspecific complexes and eliminates the possibility that these complexes are simply DNA and RNAP juxtaposed by chance.

The average lifetime of surface-bound nonspecific complexes was found to be ~600 s, which is much larger than the average lifetime of 3.3 s (Singer and Wu, 1987) and 1.5–0.1 s (Harada et al., 1999) reported for nonspecific complexes in solution under similar salt conditions. A possible explanation is that the constraints imposed by the surface slow the rates at which the complex adopts intermediate configurations required for dissociation. Dissociation rates smaller by a factor of 180 would require an increase in the activation energy leading to this intermediate by ~3.1 kcal/mol. This value is well within the range of activation energies for surface diffusion of DNA (~8.1 kcal/mol) obtained from a comparison between the diffusion constants of the DNA fragment on the surface, $D_{2D} = 7 \cdot 10^{-14}$ cm^2/s, and in solution, $D_{3D} = 5.4 \cdot 10^{-8}$ cm^2/s (Rivetti et al., 1996). Furthermore, both molecules remain in close proximity to each other for a longer time when RNAP releases the DNA, because both of them are adsorbed to the surface. Attractive interactions between the molecules might increase the probability that RNAP and DNA reassociate many times before the DNA fragment eventually dissociates completely and diffuses away. This interpretation is consistent with the observation that the lifetime of nonspecific complexes is reduced in the presence of the negatively charged DNA competitor, heparin. It is possible that the small diffusion constants and large lifetimes observed on the surface might also be observed in analogous experiments that were carried out in very viscous mediums, such as the inside of cells (Bausch et al., 1998, 1999).

Transcription

The transcription experiments showed that 40–50% of the surface-bound stalled elongation complexes, compared with ~75–80% of the complexes in solution, were able to resume transcription after addition of all four NTPs. Thus, as judged by this criterion, a large fraction of the complexes maintain their activity when being adsorbed onto the surface. However, the pattern of pauses and the termination site seem to be affected by the surface. Generally, there are many pauses because the concentration of nucleotides is only 5 μM. Several pauses are at the same sites for both complexes (for surface-bound complexes they appear to be delayed, as these complexes transcribe slower), but there are some pauses that are unique to either one of the complexes. There might be several reasons for this observation. There is evidence that RNA secondary structure, RNA interactions with the transcription complex, and the conformation of RNAP at a particular site play a crucial, regulatory role in the pattern of pauses and the termination event (Landick, 1997; Artsimovitch and Landick, 1998). It is likely that all three factors are somewhat perturbed by the surface. The surface may hamper (or stabilize) the formation of hairpins, it may influence the interactions of the transcript with the RNAP-DNA complex, and it may affect the conformation of RNAP at a particular site. Moreover, it could also be that the drag force acting on the DNA of surface-bound complexes might cause additional pauses for these complexes.

Recently, it has been shown that a hairpin in the nascent transcript is crucial for termination at the t_{R2} terminator (Yarnell and Roberts, 1999). Thus, termination for surface-bound complexes might be different, because the formation of this hairpin, or its interaction with the transcription complex, is impaired by the surface. If the hairpin is unable to interact with the transcription complex, RNAP might read through the termination site and synthesize longer than regular, full-length transcripts, as was observed in the experiments.

Frictional loading force on a transcribing RNA

An analysis of the transcription rates from the SFM sequences yielded an average value of 1.5 ± 0.8 nt/s at an NTP concentration of 5 μM. This value is in good agreement with that obtained under the same conditions in the biochemical assays (1 nt/s), and is about three to five times smaller than that measured in solution. Using the two-dimensional diffusion coefficient of free DNA molecules it is possible to estimate the average frictional drag experienced by the polymerase as it threads a DNA molecule on the surface. Because of the variability of the DNA-mica interaction among different experiments, this analysis was done using free DNA molecules in the neighborhood of a transcribing complex. Using the Einstein-Sutherland friction-diffusion relation,

$$\xi = \frac{k_B T}{D} \tag{4}$$

with $D = 1.4 \pm 0.6$ nm^2/s and $k_B T = 4.2$ pN · nm ($T = 30$°C), a value of $\xi = 3.0 \pm 0.2$ pN · s/nm is obtained. The frictional drag against which a polymerase molecule must transcribe is then

$$F = \xi v_0 \tag{5}$$

where v_o is the rate of RNA elongation. Under the conditions used in these experiments, a frictional force of 1.5 ±

0.5 pN is obtained. The frictional force estimated here represents a lower bound, since it utilizes only data for the lateral diffusion of the DNA molecules on the surface. However, RNAP must not only thread, but rotate the DNA molecule, a movement that is also hindered by the surface. The DNA helix is rotated at a speed of ~0.9 nm/s (for a DNA diameter of 2 nm). Assuming that the frictional coefficient ξ is about the same for rotation and translation, an equivalent calculation would yield an additional rotational drag force of ~2.7 pN, resulting in a total friction force of ~4.2 pN.

A recent theoretical paper has put forth a mechanical model in which RNAP is treated as a molecular motor that converts chemical energy into kinetic energy to move along the DNA (Wang et al., 1998). The model was used to calculate force-velocity curves and the stall force for RNA polymerase for different NTP or PPi concentrations. It is thus possible to predict the velocity of RNAP for a given NTP concentration and a given force acting on it. According to this model, a frictional force of ~4 pN would be required to reduce the rates from 5 nt/s to 1–1.5 nt/s at an NTP concentration of 5 μM. This number is in good agreement with the measured frictional force above, where it was assumed that RNAP has to overcome lateral and rotational friction during transcription on a surface.

Other, surface-related factors might also cause a reduction in the transcription rates. 1) Torsional strain: during transcription, positive supercoils develop in front of RNAP and negative supercoils behind it. For a linear fragment in solution, they are almost instantaneously relaxed because both helix strands can freely swivel with respect to each other. However, when the DNA strands are adsorbed onto a substrate, the relaxation of such supercoils is slowed. In this case, RNAP transcribes against an increasing torsional stress until either it stalls or the DNA lifts, at least partially, off the surface, releasing the stress before re-attaching to it. 2) Steric hindrance: RNAP may undergo conformational changes during elongation (Nudler et al., 1994), which may be necessary for transcription to proceed efficiently. Strong adsorption of RNAP to a substrate might restrict such movements and thus also reduce the transcription rate.

Recently, the viscosity, η, of the cytoplasm of macrophages and fibroblast has been found to be ~210 and 2000 Pa · s, respectively (Bausch et al., 1998, 1999). Assuming that the viscosity of the cytoplasm of *E. coli* is of the same order of magnitude (~1000 Pa · s), a molecule of the size of RNAP (r ~10 nm) experiences an in vivo frictional coefficient of $\sim\xi = 6\pi\eta r \approx 0.2$ pN · s/nm. Thus, the in vivo coefficient is much closer to the frictional coefficient that RNAP experiences in the AFM experiments (~3 pN · s/nm) than the one it experiences in standard in vitro experiments ($\sim 2 \cdot 10^{-7}$ pN · s/nm; $\eta_{water} = 10^{-3}$ Pa · s). In this sense, RNAP polymerase experiences a more realistic drag force in the present AFM experiments than it does in standard in vitro experiments. However, it should also be noted that drag force cannot be the only determining factor for the transcription rate, since the in vivo rate is higher than the rate measured in typical in vitro experiments (Uptain et al., 1997). Most likely, other factors also contribute to the high rates and fidelity of RNAP in living cells.

CONCLUSION

Transcription through-put in the cell depends on the interplay between thermodynamic and kinetic factors. The former warrant an adequate occupancy of the polymerase at the promoter, while the latter ensure both an efficient search of the target site in the midst of a large excess of noncognate DNA and appropriate elongation rates. These complex requirements determine the nature and strength of the interactions of RNAP and DNA. In this paper, the scanning force microscope has been used to investigate, in real time, the specific and nonspecific interactions of RNAP with DNA. Images of RNAP holoenzyme bound nonspecifically to promoterless DNA showed that the protein can diffuse along the DNA. This finding suggests that RNAP uses sliding to accelerate promoter location. Images of stalled elongation complexes of RNAP resuming and completing transcription upon the addition of NTPs have also been obtained. Parallel biochemical studies in solution and on the surface confirmed the rates of transcription observed for individual complexes. Further studies will benefit from improved time resolution of the instrument to better characterize elongation intermediates and the dwell times associated with pausing sites. It will also be possible to alter the conditions of deposition and modify the strength of attachment of the DNA to the surface. Following the approach demonstrated here, the diffusion coefficient of free DNA molecules in the vicinity of the elongating complexes could be used to systematically investigate the effect of increasing frictional load on the rate of transcription and pausing by RNAP as a function of NTP concentration.

We are grateful to Michael Godsey for his contributions to the RNAP sliding study.

This work was supported by National Science Foundation Grants MBC 9118482 and BIR 9318945, and National Institutes of Health Grant GM-32543. This work was supported in part by a grant from the Lucille P. Markey Foundation to the Institute of Molecular Biology. Claudio Rivetti was supported in part by an EMBO fellowship and in part by a Human Frontier Science Program (HFSP) long-term fellowship.

REFERENCES

Adam, G., and M. Delbrück. 1968. Reduction of dimensionality in biological diffusion processes. *In* Structural Chemistry and Molecular Biology. A. Rich and N. Davidson, editors. W. H. Freeman and Co., New York. 198–215.

Artsimovitch, I., and R. Landick. 1998. Interaction of a nascent RNA structure with RNA polymerase is required for hairpin-dependent transcriptional pausing but not for transcript release. *Genes Dev.* 12: 3110–3122.

Bausch, A. R., W. Möller, and E. Sackmann. 1999. Measurement of local viscoelasticity and forces in living cells by magnetic tweezers. *Biophys. J.* 76:573–579.

Bausch, A. R., F. Ziemann, A. A. Boulbitch, K. Jacobsen, and E. Sackmann. 1998. Local measurements of viscoelastic parameters of adherent cell surfaces by magnetic bead microrheometry. *Biophys. J.* 75: 2038–2049.

Berg, O., R. B. Winter, and P. H. von Hippel. 1981. Diffusion-driven mechanism of protein translocation on nucleic acids. 1. Models and theory. *Biochemistry.* 20:6929–6948.

Bezanilla, M., C. J. Bustamante, and H. G. Hansma. 1994a. Improved visualization of DNA in aqueous buffer with the atomic force microscope. *Scanning Microscopy.* 7:1145–1148.

Bezanilla, M., B. Drake, E. Nudler, M. Kashlev, P. K. Hansma, and H. G. Hansma. 1994b. Motion and enzymatic degradation of DNA in the atomic force microscope. *Biophys. J.* 67:2454–2459.

Binnig, G., H. Rohrer, C. Gerber, and E. Weibel. 1982. Surface studies by scanning tunneling microscopy. *Phys. Rev. Lett.* 49:57–60.

Bustamante, C., D. A. Erie, and D. Keller. 1994. Biochemical and structural applications of scanning force microscopy. *Curr. Opin. Struct. Biol.* 4:750–760.

Bustamante, C., M. Guthold, X. Zhu, and G. Yang. 1999. Facilitated target location on DNA by individual *E. coli* RNA polymerase molecules observed with the scanning force microscope operating in liquid. *J. Biol. Chem.* 274:16665–16668.

Bustamante, C., and D. Keller. 1995. Scanning force microscopy in biology. *Physics Today.* 48:32–38.

Bustamante, C., D. Keller, and G. Yang. 1993. Scanning force microscopy of nucleic acids and nucleoprotein assemblies. *Curr. Opin. Struct. Biol.* 3:363–372.

Bustamante, C., and C. Rivetti. 1996. Visualizing protein-nucleic acid interactions on a large scale with the scanning force microscope. *Annu. Rev. Biophys. Biomol. Struct.* 25:395–429.

Bustamante, C., J. Vesenka, C. L. Tang, W. Rees, M. Guthold, and R. Keller. 1992. Circular DNA molecules imaged in air by scanning force microscopy. *Biochemistry.* 31:22–26.

Chan, L. C., and R. Landick. 1994. New perspectives on RNA chain elongation and termination by *E. coli* RNA polymerase. *In* Transcription: Mechanism and Regulation. R. C. Conaway and J. W. Conaway, editors. Raven Press Ltd., New York. 297–321.

Craig, M. L., O. V. Tsodikov, K. L. Mcquade, P. E. Schlax, M. W. Capp, R. M. Saecker, and M. T. Record. 1998. DNA footprints of the two kinetically significant intermediates in formation of an RNA polymerase-promoter open complex: evidence that interactions with start site and downstream DNA induce sequential conformational changes in polymerase and DNA. *J. Mol. Biol.* 283:741–756.

Drake, B., C. B. Prater, A. L. Weisenhorn, S. A. C. Gould, T. R. Albrecht, C. F. Quate, D. S. Cannell, H. G. Hansma, and P. K. Hansma. 1989. Imaging crystals, polymers and processes in water with the atomic force microscope. *Science.* 243:1586–1589.

Dreier, M., D. Anselmetti, T. Richmond, U. Dammer, and H.-J. Guntherodt. 1994. Dynamic mode atomic force microscopy in liquid. *J. Appl. Phys.* 76:5095–5098.

Guthold, M., M. Bezanilla, D. A. Erie, B. Jenkins, H. G. Hansma, and C. Bustamante. 1994. Following the assembly of RNA polymerase-DNA complexes in aqueous solutions with the scanning force microscope. *Proc. Natl. Acad. Sci. USA.* 91:12927–12931.

Guthold, M., G. Matthews, A. Negishi, R. M. Taylor, D. Erie, F. P. Brooks, and R. Superfine. 1999. Quantitative manipulation of DNA and viruses with the nanomanipulator scanning force microscope. *Surf. Interface Anal.* 27:437–443.

Han, W., S. M. Lindsay, M. Dlakic, and R. E. Harrington. 1997. Kinked DNA. *Nature.* 386:563.

Han, W., S. M. Lindsay, and T. Jing. 1996. A magnetically driven oscillating probe microscope for operation in liquids. *Appl. Phys. Lett.* 69:4111–4113.

Hansma, H. G., M. Bezanilla, F. Zenhausern, M. Adrian, and R. L. Sinsheimer. 1993. Atomic force microscopy of DNA in aqueous solutions. *Nucleic Acids Res.* 21:505–512.

Hansma, P. K., J. P. Cleveland, M. Radmacher, D. A. Walters, P. E. Hillner, M. Bezanilla, M. Fritz, D. Vie, H. G. Hansma, C. B. Prater, J. Massie, L. Fukunaga, J. Gurley, and V. Elings. 1994. Tapping mode atomic force microscopy in liquids. *Appl. Phys. Lett.* 64:1738–1740.

Hansma, H. G., and D. E. Laney. 1996. DNA binding to mica correlates with cationic radius: Assay by atomic force microscopy. *Biophys. J.* 70:1933–1939.

Harada, Y., T. Funatsu, K. Murakami, Y. Nonoyama, A. Ishihama, and T. Yanagida. 1999. Single-molecule imaging of RNA polymerase-DNA interactions in real-time. *Biophys. J.* 76:709–715.

Hoh, J. H., and P. K. Hansma. 1992. Atomic force microscopy for high resolution imaging in cell biology. *Trends Cell Biol.* 2:208–213.

Kabata, H., O. Kurosava, I. Arai, M. Washizu, S. A. Marganson, R. E. Glass, and N. Shimamoto. 1993. Visualization of single molecules of RNA polymerase sliding along DNA. *Science.* 262:1561–1563.

Kadesch, T. R., R. C. Williams, and M. J. Chamberlin. 1980. Electron microscopic studies of the binding of *Escherichia coli* RNA polymerase to DNA. I. Characterization of the non-specific interactions of holoenzyme with a restriction fragment of bacteriophage T7 DNA. *J. Mol. Biol.* 136:65–78.

Kasas, S., N. H. Thomson, B. L. Smith, H. G. Hansma, X. Zhu, M. Guthold, C. Bustamante, E. T. Kool, M. Kashlev, and P. K. Hansma. 1997. *Escherichia coli* RNA polymerase activity observed using atomic force microscopy. *Biochemistry.* 36:461–468.

Kassavetis, G. A., and M. J. Chamberlin. 1981. Pausing and termination of transcription within the early region of bacteriophage T7 DNA in vitro. *J. Biol. Chem.* 256:2777–2786.

Keller, D., and C. C. Chou. 1992. Imaging steep high structures by scanning force microscopy with electron beam deposited tips. *Surf. Sci.* 268:333–339.

Landick, R. 1997. RNA polymerase slides home: pause and termination site recognition. *Cell.* 88:741–744.

Leirmo, S., and M. T. Record. 1990. Structural, thermodynamic and kinetic studies of the interaction of *Escherichia coli* σ70 RNA polymerase with promoter DNA. *In* Nucleic Acids and Molecular Biology. D. M. J. Lilley and F. Eckstein, editors. Springer-Verlag, New York. 123–151.

Levin, J. R., B. Krummel, and M. J. Chamberlin. 1987. Isolation and properties of transcribing ternary complexes of *Escherichia coli* RNA polymerase positioned at a single template base. *J. Mol. Biol.* 196: 85–100.

Lyubchenko, Y. L., A. A. Gall, L. S. Shlyakhtenko, R. E. Harrington, B. L. Jacobs, P. I. Oden, and S. M. Lindsay. 1992. Atomic force microscopy imaging of double stranded DNA and RNA. *J. Biomol. Struct. Dyn.* 10:589–606.

Lyubchenko, Y. L., and L. S. Shlyakhtenko. 1997. Visualization of supercoiled DNA with atomic force microscopy in situ. *Proc. Natl. Acad. Sci. USA.* 94:496–501.

Lyubchenko, Y. L., L. S. Shlyakhtenko, R. E. Harrington, P. I. Oden, and S. M. Lindsay. 1993. Atomic force microscopy of long DNA: imaging in air and under water. *Proc. Natl. Acad. Sci. USA.* 90:2137–2140.

Niyogi, S. K., and R. P. Feldman. 1981. Effect of several metal ions on misincorporation during transcription. *Nucleic Acid Res.* 9:2615–2627.

Nudler, E., A. Goldfarb, and M. Kashlev. 1994. Discontinuous mechanism of transcription elongation. *Science.* 265:793–796.

Putman, A. J., K. O. Van der Werf, B. G. De Grooth, N. F. Van Hulst, and J. Greve. 1994. Tapping mode atomic force microscopy in liquid. *Appl. Phys. Lett.* 64:2454–2456.

Ratcliff, G. C., D. A. Erie, and R. Superfine. 1998. Photothermal oscillation for oscillating mode atomic force microscopy in solution. *Appl. Phys. Lett.* 72:1911–1913.

Rhodes, G., and M. J. Chamberlin. 1974. Ribonucleic acid chain elongation by *Escherichia coli* ribonucleic acid polymerase. I. Isolation of ternary complexes and the kinetics of elongation. *J. Biol. Chem.* 249: 6675–6683.

Ricchetti, M., W. Metzger, and H. Heumann. 1988. One-dimensional diffusion of *Escherichia coli* DNA-dependent RNA polymerase: a mechanism to facilitate promoter location. *Proc. Natl. Acad. Sci. USA.* 85:4610–4614.

Richter, P. H., and M. Eigen. 1974. Diffusion controlled reaction rates in spherical geometry. Application to repressor-operator association and membrane bound enzymes. *Biophys. Chem.* 2:255–263.

Riggs, A. D., S. Bourgeois, and M. J. Cohn. 1970. The *lac* repressor-operator interaction. *J. Mol. Biol.* 53:401–417.

Rivetti, C., M. Guthold, and C. Bustamante. 1996. Scanning force microscopy of DNA deposited on mica: equilibration versus kinetic trapping studied by polymer chain analysis. *J. Mol. Biol.* 264:919–932.

Rugar, D., and P. K. Hansma. 1990. Atomic force microscopy. *Physics Today.* 43:23–30.

Schafer, D. A., J. Gelles, M. P. Sheetz, and R. Landick. 1991. Transcription by single molecules of RNA polymerase observed by light microscopy. *Nature.* 352:444–448.

Schlax, P. J., M. W. Capp, and M. T. Record. 1995. Inhibition of transcription initiation by *lac* repressor. *J. Mol. Biol.* 245:331–350.

Singer, P., and C.-W. Wu. 1987. Promoter search by *Escherichia coli* RNA polymerase on a circular DNA template. *J. Biol. Chem.* 262: 14178–14189.

Suh, W. C., and M. T. Record. 1993. Two open complexes and a requirement for Mg2+ to open the λPR transcription start site. *Science.* 259: 358–361.

Thomson, N. H., S. Kasas, B. Smith, H. G. Hansma, and P. K. Hansma. 1996. Reversible binding of DNA to mica for AFM imaging. *Langmuir.* 12:5905–5908.

Uptain, S. M., C. M. Kane, and M. J. Chamberlin. 1997. Basic mechanisms of transcript elongation and its regulation. *Annu. Rev. Biochem.* 66: 117–172.

Vesenka, J., M. Guthold, C. L. Tang, D. Keller, E. Delaine, and C. Bustamante. 1992. Substrate preparation for reliable imaging of DNA molecules with the scanning force microscope. *Ultramicroscopy.* 42–44: 1243–1249.

von Hippel, P. H., D. G. Bear, W. D. Morgan, and J. A. McSwiggen. 1984. Protein-nucleic acid interactions in transcription. *Annu. Rev. Biochem.* 53:389–446.

Walter, G., W. Zillig, P. Palm, and E. Fuchs. 1967. Initiation of DNA dependent RNA synthesis and the effect of heparin on RNA polymerase. *Eur. J. Biochem.* 3:194–201.

Wang, H.-Y., T. Elston, A. Mogilner, and G. Oster. 1998a. Force generation in RNA polymerase. *Biophys. J.* 74:1186–1202.

Wang, M. D., M. J. Schnitzer, H. Yin, R. Landick, J. Gelles, and S. M. Block. 1998b. Force and velocity measured for single molecules of RNA polymerase. *Science.* 282:902–907.

Yarnell, W. S., and J. W. Roberts. 1999. Mechanism of intrinsic transcription termination and antitermination. *Science.* 284:611–615.

Yin, H., M. D. Wang, K. Svoboda, R. Landick, S. M. Block, and J. Gelles. 1995. Transcription against an applied force. *Science.* 270: 1653–1657.